

1-1-2009

## Improving robotic machining accuracy by real-time compensation

Zengxi Pan

*University of Wollongong*, [zengxi@uow.edu.au](mailto:zengxi@uow.edu.au)

Hui Zhang

*University of Wollongong*

Follow this and additional works at: <https://ro.uow.edu.au/engpapers>



Part of the [Engineering Commons](#)

<https://ro.uow.edu.au/engpapers/2783>

---

### Recommended Citation

Pan, Zengxi and Zhang, Hui: Improving robotic machining accuracy by real-time compensation 2009, 4289-4294.

<https://ro.uow.edu.au/engpapers/2783>

## Improving Robotic Machining Accuracy by Real-time Compensation

Zengxi Pan<sup>1</sup> and Hui Zhang<sup>2</sup>

<sup>1</sup> Faculty of Engineering, University of Wollongong, Australia  
(Tel : +612-42215498; E-mail: zengxi@uow.edu.au

<sup>2</sup> ABB Corporate Research China  
(Tel : +86 21 6105 6370; E-mail: hui.zhang@cn.abb.com )

**Abstract:** Although robotics based flexible automation is considered as an ideal solution for foundry pre-machining operation, very few successful installations have been seen due to many major challenges involved in robotic machining processes using conventional articulated robot, such as limited material removal rate, low surface quality, and chatter/vibration. This paper explains the reasons for low surface quality in robotic machining processes and analyzes the stiffness properties of robot structure. Then a real-time compensation algorithm based on a robot stiffness model and force control scheme is introduced. The experimental results show that much better surface quality can be achieved without extending the process cycle time.

**Keywords:** robotic machining, stiffness model, real-time compensation, force control

### 1. INTRODUCTION

Industrial robots have made great contribution to factory automation and enable a reduction in the workforce. In 2008, a total of 12,557 robots valued at \$894.9 million were ordered alone in North America [1]. Nevertheless, more than 80% of the application of industrial robot is still limited in the fields of material handling and welding processes. Still very few robots have been adopted in high value-added applications such as material removal processes.

On the other hand, industry demand for cost-effective solutions of machining aluminum parts is huge. The automotive industry represents the fastest-growing market segment of the aluminum industry, due to the increasing usage of aluminum in cars. Most of the automotive aluminum parts start from casting in a foundry plant. The downstream processes usually include cleaning and pre-machining of the gating system and riser, etc., machining for high tolerance surfaces, painting and assembly.

Today, most of the cleaning and pre-machining operations are either done manually in an extremely noisy, dusty and dangerous environment or completed by dedicated CNC machines with huge capital investment. Therefore, a flexible automation solution for these operations is highly desirable. Robotics based flexible automation is considered as an ideal solution for its programmability, adaptivity, flexibility and relatively low cost, especially for the fact that industrial robot is already applied to tend foundry machines and transport parts in the process. Nevertheless, the foundry industry has not seen many successful stories for such applications and installations due to several major difficulties involved in robotic machining processes using a conventional articulated robot, such as limited material removal rate, low surface quality, and chatter/vibration. This paper will present issues and solutions for improving surface accuracy in robotic machining process.

Among the many sources of errors of machine tools, thermal deformation and geometric errors are

traditionally known as key contributors. For example, by studying a large amount of data, Peklenik [2] reported that thermal errors could contribute as much as 70% of workpiece errors in precision machining. RTEC techniques for geometric and thermal errors have successfully improved machine tool accuracy up to one order of magnitude [3, 4].

After the geometric and thermal errors are compensated for, cutting force induced errors become the major source of machine tool errors. Bajpai and Kops [5, 6] attempted to overcome the errors due to deflection using the relationship between workpiece deflection and the depth-of-cut applied at the final pass. However, most of the current error compensation research has not considered the cutting force induced errors. The following argument has been used to justify the neglect of the cutting force induced errors: in finish machining, the cutting force is small and the resulting deflection can be neglected.

However, in robotic machining process, due to the low stiffness of the industrial robot, the force induced deformation of the robot structure is the single most dominant source of workpiece surface error. An articulated robot has a much lower stiffness than a CNC machine with the similar size. Typically the stiffness of a large sized articulated robot IRB6400 is around 0.5N/ $\mu$ m compared to over 30N/ $\mu$ m for a standard CNC machine. As a result, while the robot is interacting with the environment, the position accuracy of the robot is not guaranteed due to the large contact force generated from the interaction. For example, a 500N cutting force during milling operation will cause a 1 mm position error for a robot instead of a less than 0.02mm error for a CNC machine. In order to achieve higher dimensional accuracy, the robot deformation due to the interactive force must be compensated.

Offline calibration strategies are often used to improve accuracy while sacrificing operation cycle time. The workpiece is calibrated with a distance sensor, usually LVDT or laser sensor before and after the machining process. The surface error is measured and

calculated to update the tool/workpiece data of the next cut. Although offline calibration could improve robot path error as well as force induced error, the process cycle time is increased, mostly doubled. With force sensor attached on the robot wrist, force information is ready on real time. If an accurate stiffness model could be established, the force induced error could be compensated online by updating the robot targets.

This paper is organized in six Sections. Following this introduction Section, Section two describes and compares two different robot stiffness models. The model parameters are identified in Section three. Section four presents the real-time deformation compensation method which is built up on a force control platform. Experimental results are presented in Section five. A summary and some discussions are provided in Section six.

## 2. ROBOT STIFFNESS MODELING

A robot stiffness model, which relates the force applied on the robot tool end point to the deformation of the tool end point in Cartesian space, is crucial for robot deformation compensation, since force measurement and control is fulfilled in Cartesian space while the robot position control is implemented in joint space.

The proposed model must be accurate enough for a great improvement of the surface error, as well as simple enough for real-time implementation. Detailed modeling of all the mechanical components and connections will bring a too complicated model for real-time control; and difficulties for accurate parameter identification.

The sources of the stiffness of a typical robot manipulator are the compliance of its joints, actuators and other transmission elements, geometric and material properties of the links, base, and the active stiffness provided by its position control system [7]. As commercial robotic systems are designed to achieve high positioning accuracy, elastic properties of the arms are insignificant. The dominant influence on a large deflection of the manipulator tip position is joint compliance, e.g., due to reducer elasticity [8].

The conventional formulation for the mapping of stiffness matrices between the joint and Cartesian spaces, was first derived by Salisbury [9] and generally has been accepted and applied.

$$K_x = J(Q)^{-T} K_q J(Q)^{-1} \quad (1)$$

Where  $K_q$  is a 6×6 diagonal joint stiffness matrix, which relates the motor torque load  $\tau$  on six joints to the 6×1 joint deformation vector  $\Delta Q$ ,

$$\tau = K_q \cdot \Delta Q \quad (2)$$

$J(Q)$  is the Jacobian matrix of the robot;

$K_x$  is a 6×6 Cartesian stiffness matrix, which relates the 6 D.O.F. force vector in Cartesian space  $F$  to the 6 D.O.F. deformation of robot in Cartesian space  $\Delta X$

$$F = K_x \cdot \Delta X \quad (3)$$

Eq. (1) can be derived from the definition of Jacobian matrix in Eq. (4) and the principle of virtual work in Eq. (5).

$$\Delta X = J(Q) \cdot \Delta Q \quad (4)$$

$$F^T \cdot \Delta X = \tau^T \cdot \Delta Q \quad (5)$$

For articulated robot,  $K_x$  is not a diagonal matrix and it is configuration dependent. This means: first, the force and deformation in Cartesian space is coupled, the force applied in one direction will cause the deformation in all directions; second, at different positions, the stiffness matrix will take different values.

Chen and Kao [10] introduced a more complex model using a new conservative congruence transformation as the generalized relationship between the joint and Cartesian stiffness matrices in order to preserve the fundamental properties of the stiffness matrices.

$$K_x = J(Q)^{-T} (K_q - K_g) J(Q)^{-1} \quad (6)$$

$$\text{with } K_g = \left[ \frac{\partial J^T(Q)}{\partial Q} \cdot F \right] \quad (7)$$

where  $K_g$  is a 6×6 matrix defining the changes in geometry via the differential Jacobian;  $F$  is external applied force.

The second model is more difficult to implement as the differential Jacobian is not available in the robot controller. The difference between these two models is the additional  $K_g$  in the second model.  $K_g$  accounts for the change in geometry under the presence of external load. IRB6400, a typical large sized industrial robot has a payload of 150kg, which will cause about 3 mm deformation considering its stiffness is around 0.5N/μm. From our calculation,  $K_g$  is negligible compared to  $K_q$  as this is a relative small deformation compared to the scale of robot structure.

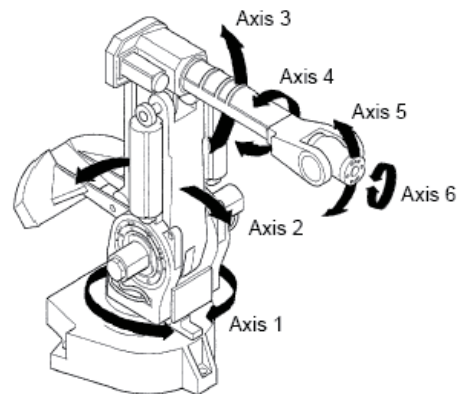


Fig. 1 Stiffness of 6-DOF ABB IRB 6400 manipulator

Thus, the conventional formulation is selected in this research for stiffness modeling. In this model, robot stiffness is simplified to six rotational stiffness coefficients, that is, equivalent torsional spring with

stiffness  $K$  as each joint is actuated directly with AC motor. Also from the control point of view, this model is the easiest to implement, since these are the 6 degree of freedom of the robot, which could be directly compensated by joint angles. Since the axis of force sensor is coincide with the axis of joint six, the stiffness of force sensor and its connection flange could be modeled into joint six. Fig. 1 shows the 6-DOF ABB IRB 6400 with black arrows represent the position of compliance joints.

### 3. PARAMETER IDENTIFICATION OF STIFFNESS MODEL

Experimental identification of the robot stiffness model parameters, joint stiffness of six joints, is critical in fulfilling real-time position compensation. In our model, the joint stiffness is an overall effect contributed by motor, joint link, and gear reduction units. It is not realistic and accurate to identify the stiffness parameter of each joint directly by disassembling the robot as the assembly process will affect the stiffness of the robot arm. The practical method is to measure it in Cartesian space.

The setup of robot stiffness measurement is shown in Fig. 2. The cutting tool at the end-effector is replaced by a sphere-tip. When robot is driven to a fixed position in the workspace, the joint angles of the robot are recorded. A weight is applied on the tool tip to generate a deformation. The position of the sphere-tip is measured by ROMOR CMM machine before and after the weight is applied to and the 3-DOF translational deformation is calculated. The applied force is measured by 6 DOF ATI force/torque sensor. A pulley is used to generate force on other directions than vertical down direction.



Fig.2 Methodology of robot stiffness measurement

Given the kinematic parameters of the robot, the Jacobian matrix at any robot position could be

calculated using robotics toolbox for MATLAB. Table 1 shows the IRB6400 kinematic model in Denavit-Hartenberg parameters.

Table 1 DH model of IRB 6400

Axis	$\theta$	d	a	$\alpha$	Home
1	$q_1$	900	188	$-90^\circ$	0
2	$q_2$	0	950	0	$-90^\circ$
3	$q_3$	0	225	$-90^\circ$	0
4	$q_4$	1300	0	$-90^\circ$	$180^\circ$
5	$q_5$	0	0	$90^\circ$	0
6	$q_6$	200	0	0	0

The same procedure is repeated at multiple positions in the robot workspace and with different loads. Table 2 shows some of the measurement data for the robot stiffness model identification procedures. From the relationship of

$$F = J(Q)^{-T} K_q J(Q)^{-1} \cdot \Delta X \quad (8)$$

$K_q$  could be solved by least square method, given  $F$ ,  $J(Q)$  and  $\Delta X$ . Only the first three equations from Eq. 8 are used in calculation as the orientation and torque are hard to measure accurately in the setup. The calibration results show that the standard deviation of the stiffness data is small, which means constant model parameter is adequate to model the deformation of robot. As shown in Fig. 3, the deviation in the entire work space is less than 0.04mm.

Table 2 Test data for stiffness model identification

Fx	Fy	Fz	dx	dy	dz
-180	0	0	-0.4561	0.1767	-0.1211
-360	0	0	-0.9232	0.2812	-0.2723
-360	0	0	-0.9604	0.2825	-0.2452
-180	0	0	-0.4822	0.1983	-0.0943
-180	0	0	-0.5359	0.2062	-0.1103
-360	0	0	-0.9775	0.3464	-0.2344
-180	0	0	-0.7276	0.0201	-0.4238
-360	0	0	-1.423	0.0073	-0.8206
-360	0	0	-1.4246	-0.0099	-0.7893
-180	0	0	-0.768	0.0184	-0.44
-180	0	0	-0.7194	0.0518	-0.4242
-360	0	0	-1.4357	0.0577	-0.7922
0	-275	25	0.0061	-0.8927	0.0336
0	-275	25	-0.0004	-0.9184	-0.0111
-40	-295	10	0.134	-1.1826	-0.0926
-40	-295	10	0.1308	-1.2146	-0.1407
-360	0	0	-0.9344	0.2758	-0.2987

### 4. REALTIME ROBOT DEFORMATION COMPENSATION

The major sources of position error in robotic machining process can be classified into two classes, (1) machining force oriented error, and (2) motion error (kinematic, measurement and servo errors, etc.). The motion error is inherent from robot position controller and will appear even in non-contact movement. While the machining force in the milling process will typically over several hundreds of Newton, the force oriented error, which will easily go up to 0.5mm, is the dominant



factor of surface error. Our objective here is to measure the deformation through a viable way and compensate it online to improve the overall machining accuracy.

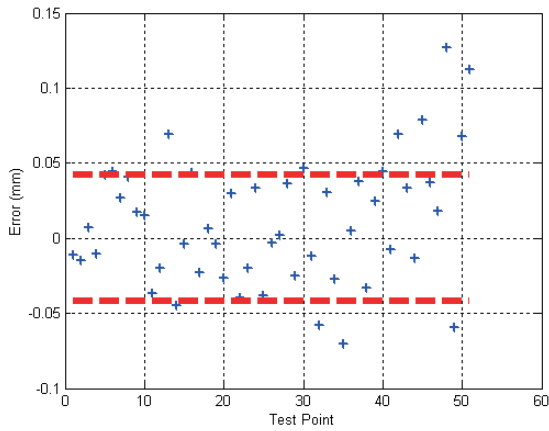


Fig.3 Deviation error of robot stiffness model



Fig.4 System Setup for Robotic Machining with Force Control (Note: This setup is using a development version of IRC5 controller. For the formal released IRC5, IRC6400 is replaced by a new IRB6640 robot.)

To our best knowledge, none of the existing research has addressed the topic of online compensation of process force oriented robot deformation due to the lack of real-time force information and limited access to the controller of industrial robot. Our research here is based on an active force control platform, which is implemented on the most recent ABB IRC5 industrial robot controller [11]. The IRC5 controller includes a flexible teach pendant with a colourful graphic interface and touch screen, which allows user to create customized Human Machine Interface (HMI) very easily. An ATI 6 DOF force/torque sensor is equipped on the wrist of the robot to close the outer force loop to realize implicit hybrid position/force control scheme.

The system setup for robotic machining with force control is shown in Fig. 4.

The block diagram of real time deformation compensation algorithm is shown in Fig. 5. After the force sensor noise is filtrated, gravity compensation must be conducted to remove the force reading from the weight of spindle and tool. Since the robot may not always maintain a wrist down position as shown in Fig. 4, a general gravity compensation algorithm is developed to remove the gravity effects for any robot configuration. The algorithm takes measurement of gravity force at 15 distinctive robot configurations and uses least square method to calculate the mass and center of mass coordinates. This information is then updated to the robot tool data and the robot will always offset the gravity from the force reading at any robot configurations.

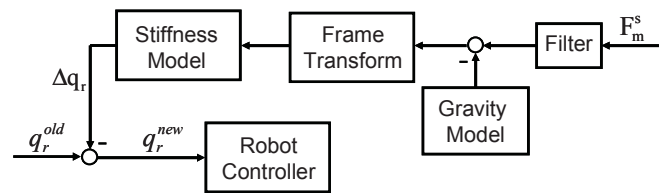


Fig.5 Block diagram of real-time deformation compensation

The force signal read from the sensor frame is then translated into the robot tool frame. Based on the stiffness model identified before, the deformation due to machining force is calculated online and the joint reference for robot controller is updated accordingly.

## 5. EXPERIMENTAL RESULTS

The experimental tests on both standard aluminum block and real cylinder head workpiece have been conducted to verify the results of proposed real-time deformation compensation method.

### 5.1 Aluminum block end milling test

A 150mm×50mm 6063 aluminum alloy block is used for end milling test. Table 3 lists the detailed parameters for the experiment.

Table 3 Parameters for end milling

Test	End milling
Spindle	SETCO,5HP, 8000RPM
Tool type	SECO Φ75mm, Square insert×6
Cutting fluid	- (Dry cutting)
Feed rate	20 mm/s
Spindle speed	3600 RPM
DOC	3 mm

A laser distance sensor is used to measure the finished surface of aluminum block as shown in Fig. 6. The surface error without deformation compensation demonstrates anti-intuitive results, on average extra 0.4mm material was removed from the aluminum block, (Fig. 7) which is not possible for a CNC machine since

the cutting force normal to the workpiece surface will always push the cutter away from the surface and cause negative surface error (cut less).



Fig.6 Setup of aluminum end milling and surface scan

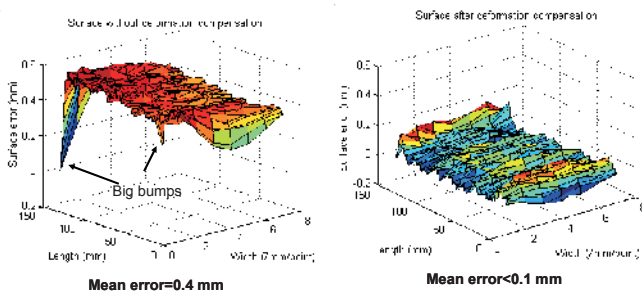


Fig.7 Deformation compensation of aluminum block  
Left: without compensation mean error=0.4mm; right: with compensation mean error<0.1 mm

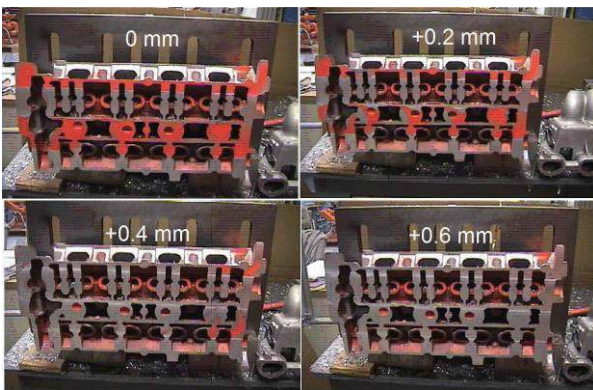


Fig.8 Cylinder head part, surface error of end milling in position control

The coupling of robot stiffness model explains this phenomenon. When end milling using square inserts, the machining force in the robot feed direction and the cutting direction (around 300N each) are much larger than the force in the normal direction (around 50N). At this specific robot configuration, the force in feed and cutting direction will both push the cutter into the workpiece, which results in positive surface error (cut more). Since the feed force and cutting force are the major components in this setup, the overall effect is that the surface is removed 0.4 mm more than commanded

depth. On the other hand, the result after deformation compensation shows a less than 0.1 mm surface error, which is in the range of robot path accuracy.

### 5.2 Cylinder head end milling test

A real cylinder head workpiece is also utilized here for deformation compensation test, using the same end milling parameters as listed in Table 2. To better visualize the surface error, the surface is covered by orange paint after the end milling. Then the tool is moved 0.1mm closer to the workpiece surface each time, until all the paint on the surface are cleaned. As shown in Fig.8 under position control, the tool touches the surface at -0.3mm, and clean the surface at 0.6mm, the total surface error is 0.9mm. Under the force control, the tool touches the surface at -0.1mm, and clean the surface at 0.3mm, the total surface error reduced to 0.4mm, as shown in Fig. 9.

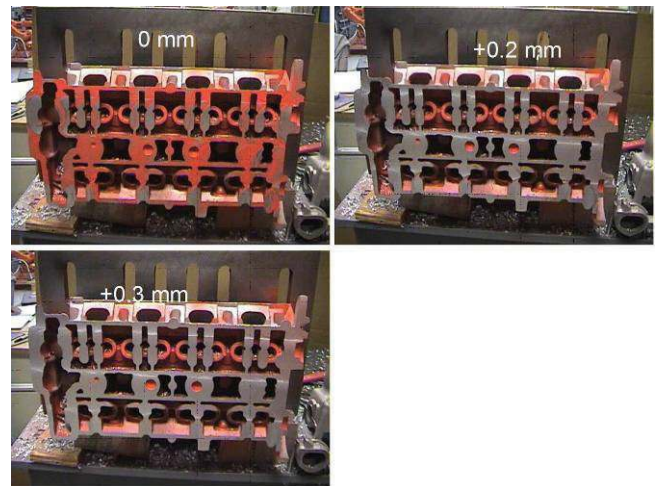


Fig.9 Cylinder head part, surface error of end milling in force control

## 6. SUMMARY AND CONCLUSION

In robotic machining process, due to the inherent low stiffness of the articulated robot, the same machining force will result in much larger deformation of the robot structure than a CNC machine. Thus the dominant source of workpiece surface error is the force induced deformation of the robot structure, which could easily reach 0.5mm in normal end milling conditions compared to 0.05mm-0.1mm of the robot position repeatability.

The coupling of the robot structure makes the problem even more complicated. Since the deformation is configuration dependent and coupled, it is very hard to predict its magnitude and direction without a proper robot stiffness model. The pattern of the robot structure deformation is related to all of the following parameters: robot configuration, the location in the work space, and the direction as well as the magnitude of the process force. Thus, it is difficult or even impossible to reduce the force induced deformation by traditional offline calibration.

In this paper, after compared with two stiffness

models for the articulated industry robot, a conventional model was used for real-time deformation estimation. The stiffness parameters were identified experimentally. The stiffness model was built in joint space with only six parameters. The simplicity of the model makes it possible for accurate identification of model parameters and implementation of real-time compensation algorithm. Although the model had not been tested throughout the entire work space, it was validated in an area large enough for machining operations.

The idea of online robot deformation compensation is to predicate the path error and update the next target position based on the measured force information, stiffness model and robot kinematics. The robot stiffness matrix has to be calculated on real-time for a good compensation accuracy since it is time varying while robot is moving.

The proposed compensation method was validated by end milling test of aluminum blocks and real cylinder head workpiece. The experimental results show that great improvement of dimensional accuracy and surface finish could be achieved. In aluminum block test the surface error decreased from 0.4mm to less than 0.1mm, and in cylinder head test it decreased from 0.9mm to 0.4mm. Generally, the deformation compensation algorithm could reduce more than 50% of force induced surface error and its highest accuracy is up to 0.1mm. As the controller compensates the next robot target based on current force measurement, the performance of the compensation is limited by the sampling time of the robot controller and the filter of the force signals.

## REFERENCES

- [1] RIA Web Site: <http://www.robotics.org>
- [2] J. B. Bryan, 1990, "International Status of Thermal Error Research", *Annals of the CIRP*, Vol. 39, No. 2, pp. 645-656.
- [3] M. A. Donmez, D. S. Blomquist, R. J. Hocken, C. R. Liu, and M. M. Barash, "A General Methodology for Machine Tool Accuracy Enhancement and Error Compensation", *Precision Engineering*, Vol. 8, No. 4, pp. 187-196.
- [4] J. S. Chen, J. Yuan, J. Ni, and S. M. Wu, "Real Time Compensation of Time-variant Volumetric Error on a Machining Center", *ASME Journal of Engineering for Industry*, Vol. 114, pp. 472-479.
- [5] S. Bajpai, "Optimization of Workpiece Size for Turning Accurate Cylindrical Parts", *International Journal of Machine Tool Design and Research*, Vol. 12, pp. 221-228.
- [6] L. Kops, M. Gould, and M. Mizrach, "A Search for Equilibrium between Workpiece Deflection and Depth of Cut: Key to Predictive Compensation for Deflection in Turning", *Proceedings 1994 ASME Winter Annual Meeting*, Vol. 68-2, pp. 819-825.
- [7] G. Alici, B. Shirinzadeh, "Enhanced Stiffness Modeling Identification and Characterization for Robot Manipulators", *IEEE Transactions on Robotics*, Vol. 21, No. 4, August 2005.
- [8] Z. Pan, H. Zhang, et al, "Chatter Analysis of Robotic Machining Process", *Journal of Material Processing Technology*, Volume 173, Issue 3, Pages 301-309, Apr 2006.
- [9] J. K. Salisbury, "Active stiffness control of a manipulator in Cartesian coordinates". *Proceedings of the 19th IEEE Conference on Decision and Control*, Albuquerque, NM, pp. 87-97, 1980.
- [10] S.F. Chen, I. Kao, "Conservative congruence transformation for joint and Cartesian stiffness matrices of robotic hands and fingers", *The International Journal of Robotics Research*, Vol. 19, No. 9, September 2000, pp. 835-847.
- [11] ABB Robot User Manual, "IRC5 Reference"